



UNIVERSITY OF LEEDS

This is a repository copy of *Effect of hydrolyzed polyacrylamide used in polymer flooding on droplet–interface electro-coalescence: Variation of critical electric field strength of partial coalescence*.

White Rose Research Online URL for this paper:  
<http://eprints.whiterose.ac.uk/149097/>

Version: Accepted Version

---

**Article:**

Yang, D, Sun, Y, Ghadiri, M [orcid.org/0000-0003-0479-2845](https://orcid.org/0000-0003-0479-2845) et al. (5 more authors) (2019) Effect of hydrolyzed polyacrylamide used in polymer flooding on droplet–interface electro-coalescence: Variation of critical electric field strength of partial coalescence. Separation and Purification Technology, 227. 115737. ISSN 1383-5866

<https://doi.org/10.1016/j.seppur.2019.115737>

---

(c) 2019, Elsevier Ltd. This manuscript version is made available under the CC BY-NC-ND 4.0 license <https://creativecommons.org/licenses/by-nc-nd/4.0/>

**Reuse**

This article is distributed under the terms of the Creative Commons Attribution-NonCommercial-NoDerivs (CC BY-NC-ND) licence. This licence only allows you to download this work and share it with others as long as you credit the authors, but you can't change the article in any way or use it commercially. More information and the full terms of the licence here: <https://creativecommons.org/licenses/>

**Takedown**

If you consider content in White Rose Research Online to be in breach of UK law, please notify us by emailing [eprints@whiterose.ac.uk](mailto:eprints@whiterose.ac.uk) including the URL of the record and the reason for the withdrawal request.



[eprints@whiterose.ac.uk](mailto:eprints@whiterose.ac.uk)  
<https://eprints.whiterose.ac.uk/>

Effect of Hydrolyzed Polyacrylamide used in Polymer Flooding on  
Droplet–Interface Electro-coalescence: Variation of Critical Electric Field  
Strength of Partial Coalescence

Donghai Yang<sup>a, b, c, \*</sup>, Yongxiang Sun<sup>a, c</sup>, Mojtaba Ghadiri<sup>b</sup>, Huanyu Wu<sup>a, c</sup>, Heming Qiao<sup>a, c</sup>,

Limin He<sup>a, c</sup>, Xiaoming Luo<sup>a, c</sup>, Yuling Lü<sup>a, c</sup>

(<sup>a</sup> College of Pipeline and Civil Engineering, China University of Petroleum, Qingdao  
266580, Shandong, PR China

<sup>b</sup> School of Chemical and Process Engineering, University of Leeds, Leeds LS2 9JT,  
UK

<sup>c</sup> Shandong Provincial Key Laboratory of Oil & Gas Storage and Transportation  
Safety, China University of Petroleum, Qingdao 266580, P R China)

Corresponding Author is Donghai Yang Tel: +86 532 86981224-86 Fax: +86 532  
86981222 E-mail: [yangdonghai12@163.com](mailto:yangdonghai12@163.com)

## Abstract

Polymer flooding is widely used in petroleum industry to enhance oil recovery. However, presence of polymer molecules in produced liquids can influence the droplet coalescence at oil–water interface in electric dehydration separators. In this study, the influence of hydrolyzed polyacrylamide (HPAM) on droplet–interface coalescence was examined through high-speed recording and observation. Deformation of droplets of aqueous polymer solution under electric fields was

experimentally observed. The images showed droplets collapsed to filament without pinch-off due to viscoelasticity. Meanwhile, fine secondary droplets erupted from the summit of filament, which was detrimental to dehydration efficiency. A critical electric field strength ( $E_{crit}$ ) beyond which partial coalescence occurred was identified. The effects of the initial droplet size, HPAM concentration, electric field waveform and frequency were explored. The results showed that  $E_{crit}$  increased with the decrease in initial droplet radius or the increase in HPAM concentration. Four kinds of AC or pulsatile electric fields (PEFs) were used including sinusoidal AC (sine AC), square, pulsed DC (PUDC) and pulsed AC (PUAC) waveforms. The increase in frequency suppressed the electro-induced stretching of droplets in the vertical direction, inhibiting partial coalescence. For these different electric fields, the increase in  $E_{crit}$  with elevated frequencies followed different ways. Overall,  $E_{crit}$  of square waveform was larger than those of other waveforms; however,  $E_{crit}$  of PUAC and sine AC waveforms may exceed that of square waveform at high frequencies. These findings are useful for the development of electro-dehydration separators for oils containing dissolved polymers in the dispersed aqueous phase.

**Keywords:** Oil–Water Separation; Droplet-Interface Coalescence; Critical Electric Field Strength; Hydrolyzed Polyacrylamide; Electric Waveform; Frequency

## **Nomenclature**

### **Abbreviation**

EOR	Enhanced Oil Recovery
HPAM	Hydrolyzed polyacrylamide
PEF	Pulsatile electric field

PUAC	Pulsed AC
PUDC	Pulsed DC
RMS	Root mean square
Sine AC	Sinusoidal AC

### **Greek symbols**

$\rho$	Density, $\text{kg}\cdot\text{m}^{-3}$
$\mu$	Viscosity, $\text{Pa}\cdot\text{s}$
$\sigma$	Interfacial tension, $\text{N}\cdot\text{m}^{-1}$
$\varepsilon$	Relative permittivity
$\varepsilon_0$	Permittivity of free space, $\text{F}\cdot\text{m}^{-1}$
$\kappa$	Conductivity, $\text{S}\cdot\text{m}^{-1}$

### **Roman symbols**

A	The projected area of the droplet, $\text{m}^2$
$C_d$	Drag coefficient
E	Electric field strength, $\text{kV}\cdot\text{m}^{-1}$
$E_{\text{crit}}$	Critical electric field strength, $\text{kV}\cdot\text{m}^{-1}$
$f_0$	Natural frequency of polymer droplets, Hz
$F_B$	Buoyancy force, N
$F_D$	Drag force, N
$F_E$	Electric force, N
g	Gravitational acceleration, $\text{m}\cdot\text{s}^{-2}$
H	Thickness of Phase layer, m
$H_{\text{peak}}$	Characteristic height of the droplet, $\mu\text{m}$
G	Gravity force, N
k	Slope of $E_{\text{crit}}$ and $R^{-0.5}$ , $\text{v}\cdot\text{m}^{-0.5}$
$\Delta P$	Difference in the additional pressure, N
R	Radius, m
U	Applied voltage, V
v	Relative velocity of a droplet falling in oil, $\text{m}\cdot\text{s}^{-1}$

$V_d$  Volume of the droplet,  $m^3$

### **Super/subscripts**

1 Aqueous phase

2 Oil phase

## **1. Introduction**

### **1.1 EOR additive HPAM may affect the electro-dehydration of emulsion**

Polymer flooding is an important chemical enhanced-oil-recovery technique, the first field-test of which was conducted in USA as early as 1964. In recent years, with oil price recovery worldwide, improvement of polymer flooding technology, and reduction of its cost, the focus on polymer flooding is renewed [1]. According to statistics, polymer flooding could improve the recovery rate by 5%-30% [1-5]. Oil trapped in dead ends of pores in oil rocks could be pulled out by aqueous polymer solutions. In particular, polymers could increase the volumetric sweep and displacement efficiency of injected water due to enhanced viscosity and reduced water/oil mobility ratio [1, 6]. Some studies also reported that the viscoelastic nature of the polymers can elevate displacement efficiency [1, 4]. Kamal et al. [1] summarized the polymer types used in nearly 20 oil fields, including Daqing, Pelican, and West Khel. Due to relatively low-temperature and low-salinity properties of most of these reservoirs, HPAM is widely employed in oil fields [1, 4]. HPAM belongs to anionic polymers. The negative charge induced by hydrolysis would increase repulsion between the HPAM chains and yield HPAM solutions with increased viscosities [1]. In addition, aqueous HPAM solutions also exhibit significant viscoelasticity [4, 7].

In Daqing oilfield, 30%~50% of injected polymer would be re-extracted to the ground with the produced liquid after polymer flooding [6]. Due to a series of shearing during oil extraction and gathering processes, the produced liquid would form a stable emulsion, which needs to be dehydrated to meet the requirement of water content of commercial crude oil [8, 9]. Commonly, the dehydration methods include natural sedimentation, centrifugal settling, chemical demulsification, electrostatic dehydration, and membrane demulsification, etc. [10]. Of them, electro-dehydration method is used for separating water-in-oil emulsions during oil processing, and can effectively reduce the water content of oil to below 0.5% [8, 11]. However, it is reported that produced liquids containing polymer molecules are difficult to be treated in many oilfields [12, 13]. In view of this, the macroscopic background of this study is to investigate the impacts of polymers on the electro-dehydration of emulsion.

## **1.2 An important pattern of electro-dehydration: droplet–interface coalescence**

Horizontal electric dehydration separator is the dewatering facility generally used in oilfield gathering and transportation system. Water-in-oil emulsions entering the electrostatic separator would stay for some time depending on the designed throughput. During this time, part of water will settle to the bottom, forming an oil–water interface [14]. Then, the subsequent settled water droplets will stay at the interface for a while and eventually merge into the underlying bulk phase through droplet–interface coalescence. Microscopically, droplet–interface coalescence can be divided into several steps: thinning and rupture of film between droplets and interface,

and coalescence [15-17].

### **1.2.1 Partial coalescence is undesirable for electro-dehydration**

The application of external electric fields affects droplet–interface coalescence. Due to the difference in permittivity between the oil and aqueous phases, polarisation of the aqueous phase becomes possible [18]. Therefore, droplets are subjected to electrostatic forces in an electric field. On one hand, the electrostatic force between the droplets and interface accelerates the rupture of the oil film, promoting the occurrence of coalescence [8, 14, 19, 20]; on the other hand, it stretches the droplets following the charge transfer when the droplet touches the interface, which may retard the coalescence and help to pull away of the droplets from the interface [16, 21]. At high electric field strengths, the upward stretching force can cause the breakage of the droplets. The droplets split and leave fine secondary droplets, a phenomenon known as partial coalescence. Obviously, partial coalescence is undesirable for electrostatic dehydration as it makes the remove of smaller droplets more challenging. Therefore, prevention of partial coalescence merits further studies.

### **1.2.2 Research status of factors influencing partial coalescence**

The literature search revealed that both electric field and physical factors of liquids influence the occurrence of partial coalescence [16, 22-28]. In particular, higher electric field strengths are conducive to form larger secondary droplets [25, 26]. The increase in radii of initial droplets may promote the occurrence of partial coalescence [16, 23, 28]. Aryafar et al. [23] found that the use of a high viscosity oil or coalescing droplet with a low permittivity is not conducive to induce partial

coalescence. Impurities in the aqueous phase also affect the coalescence results. This was simulated by addition of relevant chemicals. Mousavichoubeh et al. [16] noted that hydrophilic surfactants significantly reduced the oil–water interfacial tension, thus promoting the formation of larger secondary droplets. Vivacqua et al. [27] suggested that increasing conductivity of water to a certain range through addition of salts could suppress partial coalescence. Harbottle et al. [29] presented that the increment of nanoparticle concentration in the water droplets transforms the coalescence from partial to complete.

AC or pulsatile electric fields are used in electric dehydrators to avoid short circuits between electrodes, especially when processing water-in-oil emulsions with high water content. The effects of electric field waveforms and frequencies on droplet–interface coalescence are studied. For instance, Mousavi et al. [25] investigated the influence of square, sawtooth and half-sinusoidal waveforms on droplet–interface coalescence, and reported sawtooth waveform as the most effective waveform in reducing secondary droplets volumes. Vivacqua et al. [30] studied the influence of the same waveforms on electrocoalescence of water drop trains and obtained similar results. Elevated frequencies suppressed the formation of secondary droplets [25].

### **1.3 Research status of the coalescence of polymer-containing droplets**

Research works on the electro-coalescence of polymer-containing droplets have hitherto focused on the motion and deformation of single droplets, or the coalescence between binary droplets. Luo et al. [31] studied the natural floating motion of oil

droplets in HPAM solutions in the buoyancy field, and noticed that cross-link structures formed by HPAM molecules and increased water viscosity were responsible for decreasing oil droplets floating velocities. Yan et al. [32] investigated the deformation of HPAM-containing droplets under electric fields. Their experimental results illustrated that the interfacial tension and the elasticity of the non-Newtonian fluid are pronounced for deforming polymer droplets. Verdier [33] explored the coalescence of polymer droplets under the influence of van der Waals forces only to determine the relationship between various combinations of droplets viscosities and characteristic time of coalescence. However, droplet–interface electro-coalescence containing polymers has not been addressed widely. Yang et al. [28] preliminarily investigated the effect of polymers on the coalescence of droplets at oil–water interface subjected to DC electric fields, and observed that adding polymers to water raised the critical electric field strength for the occurrence of partial coalescence.

Overall, HPAM can yield complex aqueous phase behavior. The study of its effect on droplet–interface coalescence, especially on  $E_{crit}$  for the occurrence of partial coalescence, is ongoing but not sufficient. In this study, the effects of initial droplet size, HPAM concentration, electric field waveform and frequency on  $E_{crit}$  are experimentally determined for the occurrence of droplet–interface partial coalescence. The outcomes of the current work would be useful for optimizing the application of electro-dehydration separator for polymer-containing oil-water emulsions.

## 2. Experimental methodology

### 2.1 Experimental set-up and procedure

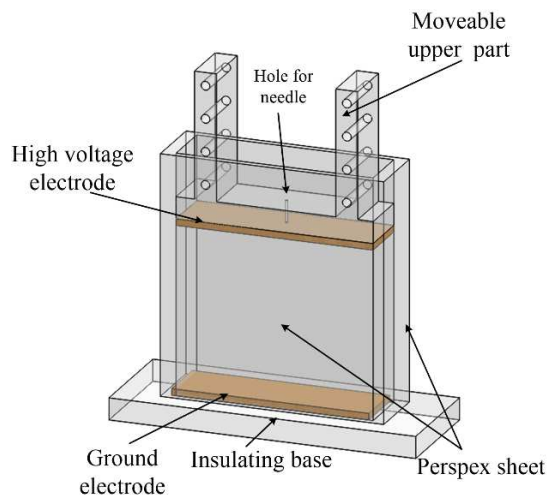


Fig. 1 Schematic of the test cell used in the experiment

The experimental cell was the same as that used by Mousavichoubeh et al. [16, 26]. As shown in Fig. 1, two polished brass plates with dimensions of 90 mm  $\times$  25 mm, as the electrodes, were placed parallel in the experimental cell. The high voltage electrode was attached to an insulating slider. A hole with a diameter of 1 mm at the center of the slider and the high voltage electrode enabled the injection of droplets into the continuous oil phase. The ground electrode was attached to the insulating base. The distance between the electrodes could be adjustable by moving the slider up or down.

Two layers of immiscible liquids were added to the experimental cell to simulate the planar oil–water interface in the horizontal electric dehydration separator. The bottom half of the cell was filled with HPAM aqueous solutions and the top half was filled with silicon oil. Then, droplets were injected into the cell through the hole, by using a hypodermic needle attached to a syringe (Hamilton micro-liter syringe). The

needle was grounded in the absence of any electric field to ensure droplets are uncharged. The injected droplet fell down slowly until it rested at the interface. By applying an electric field, the coalescence would occur rapidly. This process was recorded by high-speed digital video recording using Photron FASTCAM SA5 camera equipped with a micro lens (NAVITAR 12× Zoom Lens). A halogen cold lamp (Dedolight DLHM4-300) with four flexible fibre optic heads was used for lighting to high speed recording. The images taken were analyzed by the image processing software Image J and PFV (Photron Fastcam Viewer ver. 320) software.

## 2.2 Types of electric signal used in experiments

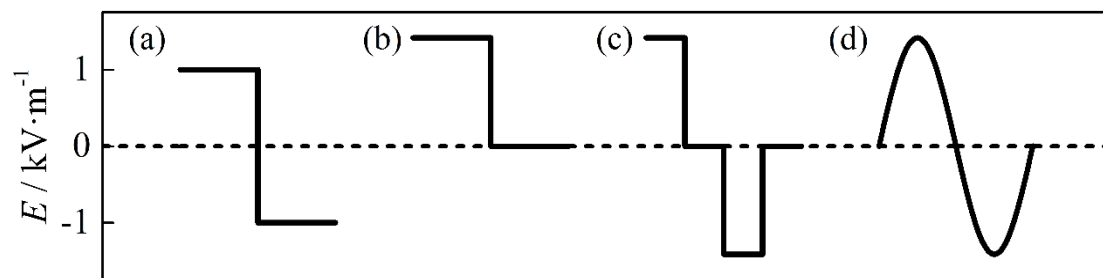


Fig. 2 The sketch of different types of AC or pulsed waveforms used in the experiment: (a) Square waveform, (b) PUDC waveform, (c) PUAC waveform, and (d) Sine AC waveform. The bold solid lines show the periodic characteristics of different waveforms (one period) and the dotted line represents the axis where  $E$  is equal to 0.

Five different electric waveforms were generated by a signal generator (Tektronix AFG1022), including DC, square, PUDC, PUAC, and sine AC waveforms. Fig. 2 shows the periodic characteristics of AC or pulsed waveforms used in experiments. Electric signals were amplified 2000 times by the high voltage power amplifier (TREK 20/20C), with a maximum output voltage of 20,000 V. To express the effectiveness of the different waveforms, the RMS value of the field strength is

commonly used, which corresponds to the value of a DC voltage giving the same electrical power [30, 34, 35]. The RMS value was also used in this work. In addition, due to the discontinuity of the dielectric constant of oil and water, the electric field strength  $E$  in oil is given by [36]:

$$E = \frac{U}{(H_2 + H_1 \frac{\epsilon_2}{\epsilon_1})} \quad (1)$$

### 2.3 Preparation of experimental liquids

HPAM can be prepared by a commonly manufacturing processes: hydrolysis of polyacrylamide (PAM). The reaction is shown in Fig. 3. In this work, commercial HPAM was provided by PetroChina DaQing Refining & Chemical Company, with a relative molecular weight of  $300 \times 10^4$  to  $500 \times 10^4$  and a degree of hydrolysis of less than 30 %. The silicon oil was purchased from Sigma-Aldrich. According to Sheng et al. [4] review, the amount of polymer injected from all the surveyed polymer projects with available data was in the range of 0 ~ 900 ppm·PV. Based on this, the range of HPAM concentrations was from 0 ppm to 600 ppm used in the experiments in this work. The properties of the silicon oil and HPAM solutions are given in Table 1. The conductivity of polymer solutions was measured by using a conductivity indicator (Model 4310, Jenway Products Inc), and the conductivity of oil was measured by an oil conductivity meter (GD29YX1154B). The viscosities of oil and polymer aqueous solution were measured using the Bohlin CVO rheometer (Malvern Instruments Inc). Moreover, density was measured by using a volumetric flask and interfacial tension was measured using the contact-angle measuring instrument EasyDrop (Kruss GmbH Inc).

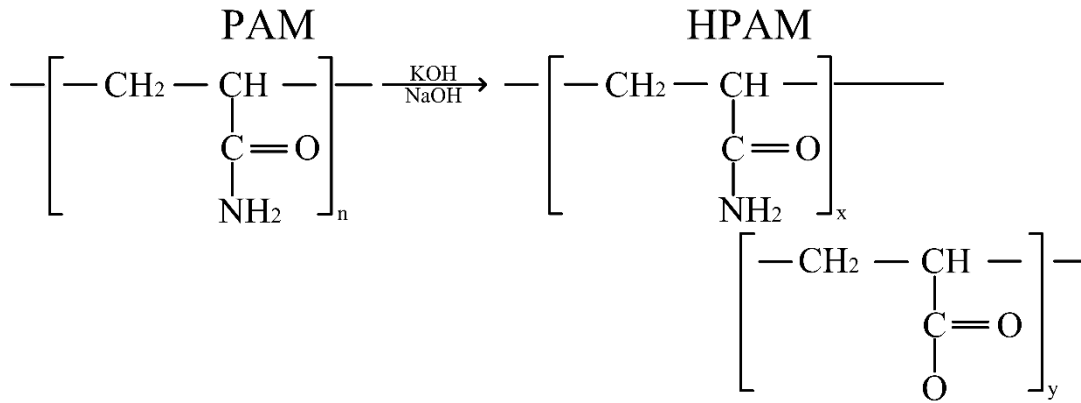


Fig. 3 Molecular structure of PAM and HPAM [36].

**Table 1 Properties of silicon oil and HPAM solution used in experiments**

Liquids	Conductivity ( $\mu\text{S}\cdot\text{cm}^{-1}$ )	Viscosity ( $\text{mPa}\cdot\text{s}$ )	Density ( $\text{kg}\cdot\text{m}^{-3}$ )	Interfacial tension ( $\text{mN}\cdot\text{m}^{-1}$ )
Silicon oil	$2.32\times 10^{-7}$	56.99	950	-
Distilled water	1	1.27	998	39.81
HPAM 50ppm	18.88	5.93	998.24	31.01
HPAM 100ppm	31.4	9.48	998.52	30.56
HPAM 200ppm	67.4	17.45	998.68	29.71
HPAM 400ppm	109.2	28.31	999.94	28.33
HPAM 600ppm	145.4	36.81	1000.92	27.34

### 3. Results and discussion

When the droplet coalesces at an interface under an electric field, the coalescence form is determined by the forces exerted on the coalescing droplet. Due to the dynamic change in droplet shape during coalescence, it would be difficult to give the magnitude of the forces at each moment. However, at the very beginning of the coalescence when the droplet can be considered to remain spherical, the forces can be analyzed. The difference in the additional pressure  $\Delta P$  between the coalescing droplet and bulk phase mainly drives the coalescing droplet to discharge its liquids into the bulk [16, 26, 38]. In general, the additional pressure of bulk phase could be

neglected because the radius of curvature of the interface tends to infinity. Hence,  $\Delta P$  is approximately equal to the addition pressure of a spherical droplet, given by Young-Laplace equation  $\Delta P = \frac{2\sigma}{R}$ . An electric field force  $F_E$  will pull the droplet upward to hinder the droplet from merging completely into the bulk phase, and  $F_E$  can be calculated as  $F_E = 6.58\pi\epsilon_0\epsilon_2 R^2 E^2$  [18, 39, 40]. For a spherical droplet falling in the surrounding oil, the drag force  $F_D$  is given by Chiesa et al. [41],  $F_D = \frac{1}{2}\rho_2 C_d A v^2$ . Furthermore, the difference between the gravity force  $G$  and buoyancy force  $F_B$  can be expressed as  $G - F_B = (\rho_1 - \rho_2)gV_d$ . Therefore, all the physical factors (including  $R$ ,  $\sigma$ ,  $\rho$ , etc.) and electric field factors (including  $E$ , etc.) can affect the coalescence. In the practical application of electric dehydration separator, the adjustable factor is usually the applied electric field strength  $E$ . With the change in  $E$ , different coalescence forms can be achieved, as analyzed below for the influence of the presence of dissolved polymer in the aqueous phase.

### **3.1 Coalescence behaviors of the polymer-containing droplet**

#### **3.1.1 Different forms of droplet-interface coalescence**

Fig. 4 (a) indicates that in the absence of an electric field or in the presence of low electric field strengths, the coalescing droplet could fully merge into the bulk, inducing complete coalescence. As the field strength is increased, the liquid bridge breaks up before reaching complete coalescence, leading to partial coalescence. This leaves the main secondary droplet and a train of fine droplets above the interface (Fig. 4 (b)). Some of fine droplets are not visible in print. Both observed patterns are

conventional in droplet–interface coalescence, not only for polymer droplets as used here but also for droplets containing surfactants, ions, among others.

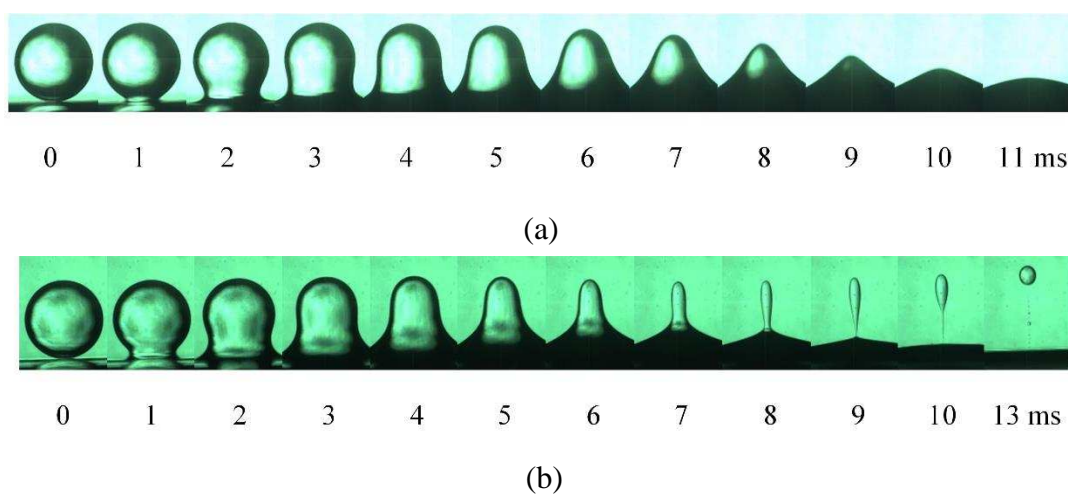
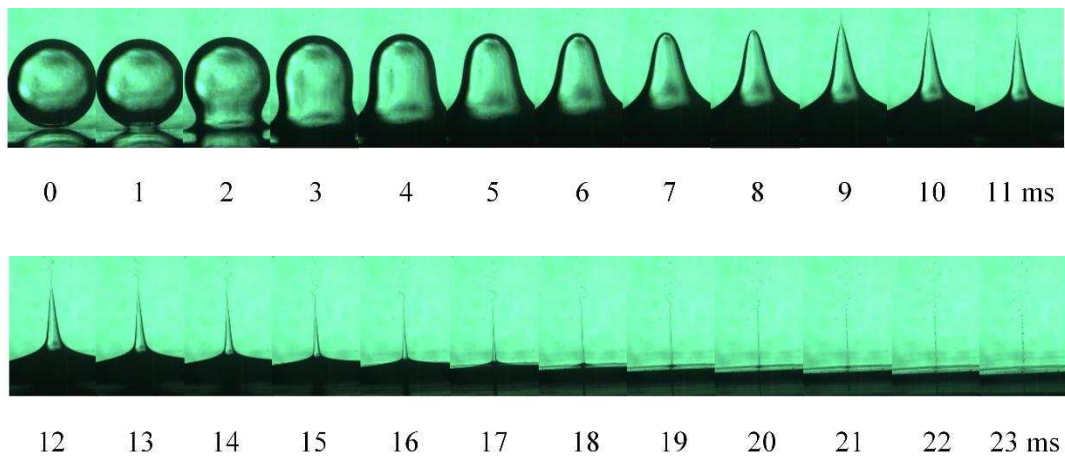


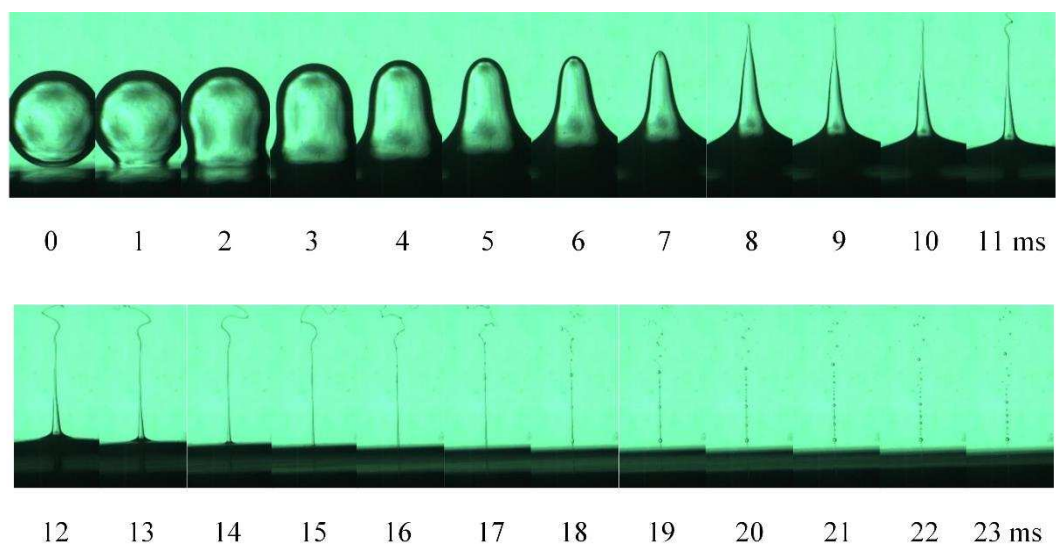
Fig. 4 Conventional patterns of droplet–interface coalescence. (a) Complete coalescence of a droplet with radius of  $640\ \mu\text{m}$  subjected to a DC electric field with amplitude of  $310.6\ \text{kV}\cdot\text{m}^{-1}$  (concentration of HPAM solution is 600 ppm), and (b) Partial coalescence of a droplet with radius of  $640\ \mu\text{m}$  subjected to a DC electric field with amplitude of  $483\ \text{kV}\cdot\text{m}^{-1}$  (concentration of HPAM solutions is 50 ppm).

Polymer solutions usually exhibit the viscoelastic properties under severe stretching and deformation, as it is the case of the droplet during coalescence, which influences the formation of secondary droplets. It has been reported that the viscoelasticity of polymer solutions suppresses partial coalescence in the absence of electric fields [42]. In fact, viscoelastic effects would only be triggered when the polymers are extensively stretched [43]. In our experiments, the polymer droplet brought out interesting viscoelastic effects at relatively high field strengths. As shown in Fig. 5 (a), the shape of the coalescing droplet is stretched from initial sphere to a liquid column by the upward electric field force. A short filament is pulled out from

top of the liquid column, disintegrating into fine droplets and getting dispersed into the surrounding oil. As the liquid column gradually collapses, the filament becomes longer; meanwhile, the filament continues stretching and discharging its liquids in the form of fine droplets. Its height eventually starts decreasing due to the eruption of fine droplets. As the height decrease to a certain size, the filament breaks up into several droplets from the bottom and thinnest positions along the filament, very similar to break-up of ‘beads-on-string’ structures (Fig. 6) for viscoelastic jets. As shown in Fig. 6, several droplets are connected by the thin filaments between them which will eventually break at the thinnest positions. As the concentration of the polymer solution and field strength is further increased, the filament forms earlier and becomes longer but more difficult to break (Fig. 5 (b)). In some extreme cases, no breakage of the filament from the bottom is observed during the entire coalescence period.



(a)



(b)

Fig. 5 The formation of a filament by the polymer-solution droplet under DC electric field, for (a)  $R$  is  $598\ \mu\text{m}$  and  $E$  is  $578\ \text{kV}\cdot\text{m}^{-1}$ ; concentration of polymer solution is  $200\ \text{ppm}$ , and (b)  $R$  is  $598\ \mu\text{m}$  with the same polymer concentration as case (a), and  $E$  is  $607\ \text{kV}\cdot\text{m}^{-1}$ . (The more detailed processes are shown in Supplementary materials 1 and 2, respectively)

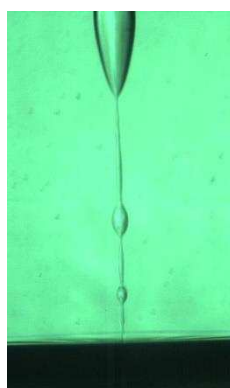


Fig. 6 A typical beads-on-string structure observed in experiments. (The initial droplet with radius of  $640\ \mu\text{m}$  subjected to a DC electric field with amplitude of  $535\ \text{kV}\cdot\text{m}^{-1}$ ; concentration of HPAM solutions is  $50\ \text{ppm}$ )

### 3.1.2 Analysis of the breakup mechanism of droplets

The above coalescence phenomena observed in the experiments reflect the complexity of droplet–interface coalescence containing polymers. For a droplet of a polymeric solution, there are two coalescence modes: 1) the conventional coalescence mode, 2) the viscoelastic mode, in which the droplet undergo extensive reversible stretching and delayed pinch-off [42, 44]. The applied electric field is mainly responsible for stretching the droplet, and the corresponding reaction of polymer molecules inside the droplet should play a role in switching between the two modes. The deformation and breakup of an extended droplet in an otherwise quiescent fluid was attributed to the Rayleigh instability [45]. This mechanism described that the droplet would be unstable due to a natural growth of finite-amplitude capillary disturbances [45, 46, 47]. However, capillary-wave instabilities at the fluid-fluid interface have been observed only for highly elongated drops [48]. For the conventional coalescence process, the finite interfacial tension of the interface should drive the motion leading to breakup [16, 21, 48], which occurs on a much shorter timescale than the growth of capillary waves [47, 48, 49]. H.A. Stone et al. [48, 49] simulated the pressure distribution in the extended droplets with a bulbous end. As shown in Fig. 7 (a), due to the change of interface curvature, the capillary pressure gradient induces flow both from the end of the drop and from the central cylindrical region. The high initial curvature at the bulbous end tend to cause large velocities near the end and a reduction in droplet length [49]. The end gradually bulb up which lowers the pressure in this region. Meanwhile, the pressure-driven flow away from the cylindrical region leads to the development of a neck and, consequently, a local

pressure maximum, which will eventually result in droplet breakup via the capillary pinch-off process [48, 49].

For the viscoelastic mode, as the polymer molecules are strongly stretched, tensile strength will be developed in the droplet filament to suppress the capillary pinch-off. Simulations performed by Li et al. [43] showed that variations in axial elastic forces in the filament is roughly four times larger than those of capillary forces with opposite sign. As the filament becomes longer and thinner, the rapid growth of axial elastic stress prevents the filament from further necking. Other experiments also depicted that the time of the breakup of viscoelastic jets is several orders of magnitude longer than that of Newtonian jets [43, 50, 51]. However, in the end of the filament, the filament is strongly stretched to form the “pointed end”. The strong electric field force may break the original balance between internal and external forces on the filament, and the capillary pinch-off occurs. The “pointed end” quickly retracts, thus transforming the end into a bulbous shape (Fig. 7 (b)). The subsequent multiple satellite formation is self-repeating in the sense that every pinch-off is always associated with the formation of a neck, the neck undergoes an additional pinch-off, and the process repeats at smaller scales [46]. It is worth noting that in the final stage of filament fracture, an abrupt appearance of finite-amplitude waves on the remaining thread leads to simultaneous breakup into a line of small drops (Fig. 6). This abrupt occurrence of capillary-wave instabilities indicates that the prolongation of time required for droplet breakup provides sufficient time for the growth of capillary disturbances. At present, the behavior of polymer-containing droplets in coalescence

cannot be fully explained, and in-depth breakup mechanism of the viscoelastic thread under electric fields requires further studies.

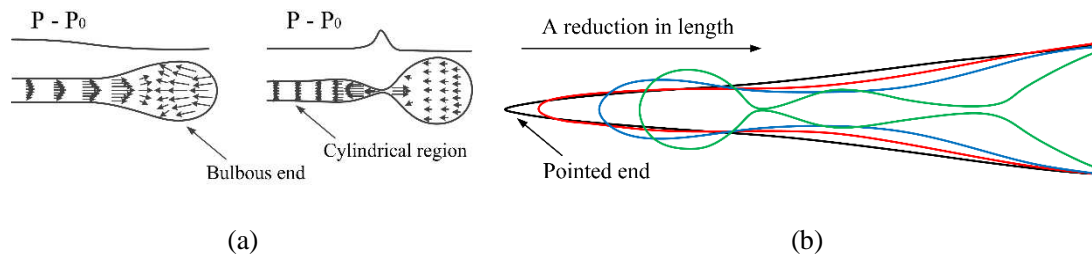


Fig. 7 (a) Velocity and pressure fields for an extended droplet during the breakup process. The pressure field  $P - P_0$  shown is the droplet pressure along the centerline and  $P_0$  is the pressure at the droplet center [49]. (b) Sketch of the formation of multiple satellites from the droplet filament [46].

Overall, the existence of polymer in the aqueous phase during droplet–interface coalescence may extend the coalescence time and also form a large amount of fine secondary droplets. Whether partial coalescence would proceed in viscoelastic mode or just in conventional mode may depend on many factors, such as concentration of polymer solutions and applied electric field strength. However, partial coalescence would always be detrimental to electric dehydration, and therefore its mitigation is highly desirable when using electro-dehydrators to process water-in-oil emulsions in oil industry. In the experiments, partial coalescence only initiated above a critical electric field ( $E_{crit}$ ). To determine  $E_{crit}$ , the output voltage between the electrodes was adjusted under the minimum adjustment range allowed by the experimental equipment ( $\pm 2$  V). As the applied electric field strength gradually approached  $E_{crit}$ , only a short filament is pulled up before the coalescing droplet completely merge into the bulk phase, and therefore the secondary droplet formed in partial coalescence

would be very small (Fig. 8). Once the coalescence just transformed from partial to complete (Fig. 4 (a)), the voltage was recorded and the corresponding electric field strength was taken as  $E_{crit}$ . In the following, the effects of initial droplet radius, concentration of HPAM polymer solution, electric waveform and frequency on  $E_{crit}$  are all discussed.

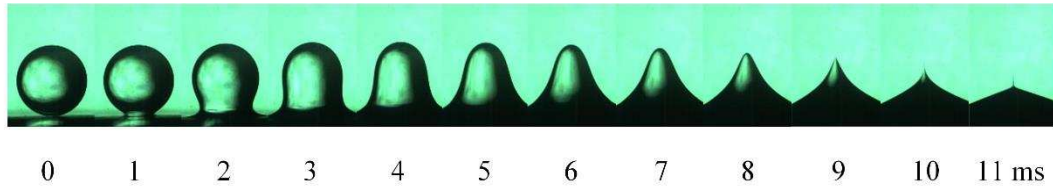


Fig. 8 The state of the coalescence when the applied electric field strength approaches  $E_{crit}$ . (The initial droplet with radius of 546  $\mu\text{m}$  subjected to a DC electric field with amplitude of  $723 \text{ kV}\cdot\text{m}^{-1}$ ; concentration of HPAM solutions is 600 ppm)

### 3.2 Influences of initial droplet radius and HPAM concentration on $E_{crit}$

In Fig. 9 (a),  $E_{crit}$  decreases as initial coalescing droplet size is increased. As analyzed above, the increase in  $R$  reduces  $\Delta P$ , thereby reducing the initial kinetic energy that drives the liquids in the droplet into the bulk. Furthermore, large initial droplets are subjected to large electric field forces  $F_E$ , as well as drag forces  $F_D$ , which are conducive to the occurrence of partial coalescence. Therefore, the synergistic effect of these will lead to the decrease of  $E_{crit}$ .

Several formulas have been proposed to calculate  $E_{crit}$  for breaking, such as  $E_{crit} = \sqrt{\frac{C\sigma}{\varepsilon_0\varepsilon_2R}}$  for single conducting droplet [40], and  $E_{crit} = \sqrt{\frac{2\pi\sigma}{\varepsilon_0(\varepsilon_1-\varepsilon_2)R}}$  for a liquid jet [52].  $E_{crit}$  of both is proportional to  $R^{-0.5}$ , indicating possible similarities between different patterns of liquids breakup. In our experiments,  $E_{crit}$  follows a nearly linear trend with the reverse of square root of droplet radius ( $R^{-0.5}$ ) (Fig. 9 (a)). Fig. 9 (b)

shows that the slope  $k$ , given by the ratio  $(E_{crit} / R^{-0.5})$ , increases with the increase of HPAM concentration.

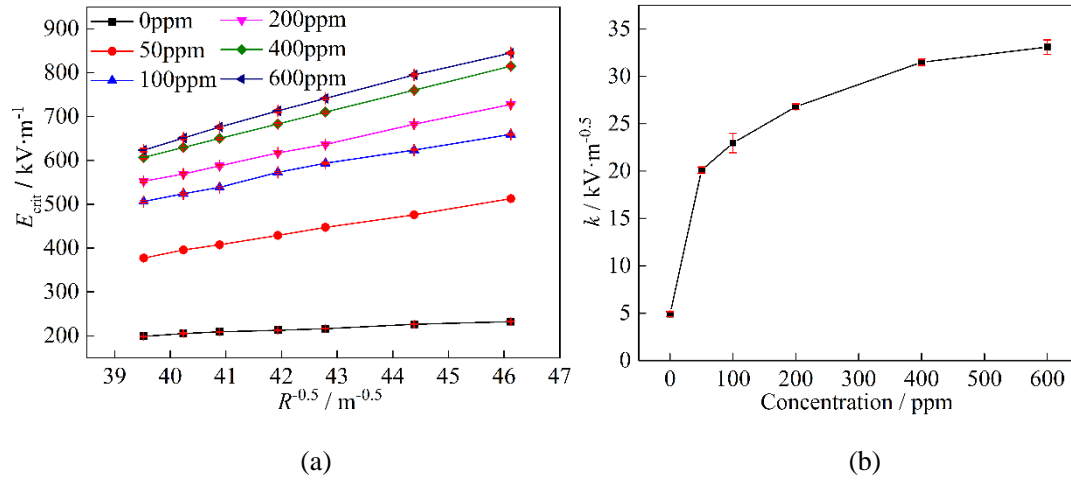


Fig. 9 (a) the effect of  $R$  on  $E_{crit}$  under square electric fields with a frequency of 1 Hz, and (b) the relationship between the slope  $k$  of the lines given by  $(E_{crit} / R^{-0.5})$  and the concentration of polymer solution.

As HPAM concentration increases,  $E_{crit}$  becomes larger and sensitive to the size of initial droplet. As reported in our previous studies, polymer molecules could form cross-link structures in aqueous phase with tighter structures at higher concentrations [31]. Therefore, such structures could enhance viscoelasticity of the droplet. The tensile strength due to viscoelasticity can delay pinch-off of the droplet [53]. Stretching of the polymer chains along the axis can lead to long extension of the droplet without breaking (Fig. 5). Once the electric field is turned off, the surface of droplet will quickly shrink to recovery its shape. The experimental findings by Chen et al. [42] also reveals that polymer drops tend to generate smaller secondary droplets in the absence of electric fields. Therefore, the addition of HPAM may inhibit the occurrence of partial coalescence, resulting in increased  $E_{crit}$ . Furthermore, the

conductivity and viscosity of aqueous phase increases as HPAM concentration is increased; in contrast, the oil–water interfacial tension only slightly reduces (Table 1). It has been reported that the formation of secondary droplets can be avoided if the water conductivity is increased within a certain range [27]; moreover,  $E_{\text{crit}}$  also increases at elevated conductivities [28]. The increase in droplet viscosity ( $\mu_1$ ) can lead to two competing effects: damping of the rate of drainage of the aqueous liquid into the continuous aqueous phase and prolonging the coalescence time [53]. The simulations of Yue et al. [53] shows that the volume ratio between secondary droplets and the initial droplet increases and then declines as the droplet viscosity increases. The effect of the increased droplet viscosity on partial coalescence is difficult to discern from our experiments.

### **3.3 Influence of electric frequency on $E_{\text{crit}}$ for different electric waveforms**

To prevent shortcomings of application of DC electric fields, such as short circuit and corrosion, AC or pulsatile electric fields (PEFs) have been widely employed. The coalescence under PEF is closely related to the frequency. As shown in Fig. 10, the coalescence pattern transforms from partial to complete as frequency is increased. Fig. 11 depicts the variation in the characteristic height of the droplet during coalescence for different frequencies. In droplet–interface coalescence, the electric field force  $F_E$  stretches the droplet upward, thereby delaying the merging of the droplet into the continuous phase. However, as the frequency increases, the change in droplet height is suppressed, reducing and ultimately eliminating the stretching effect of the electric force on the droplet. Therefore, partial coalescence can be inhibited by increasing the

frequency without short-circuiting, as  $E_{\text{crit}}$  increases too.

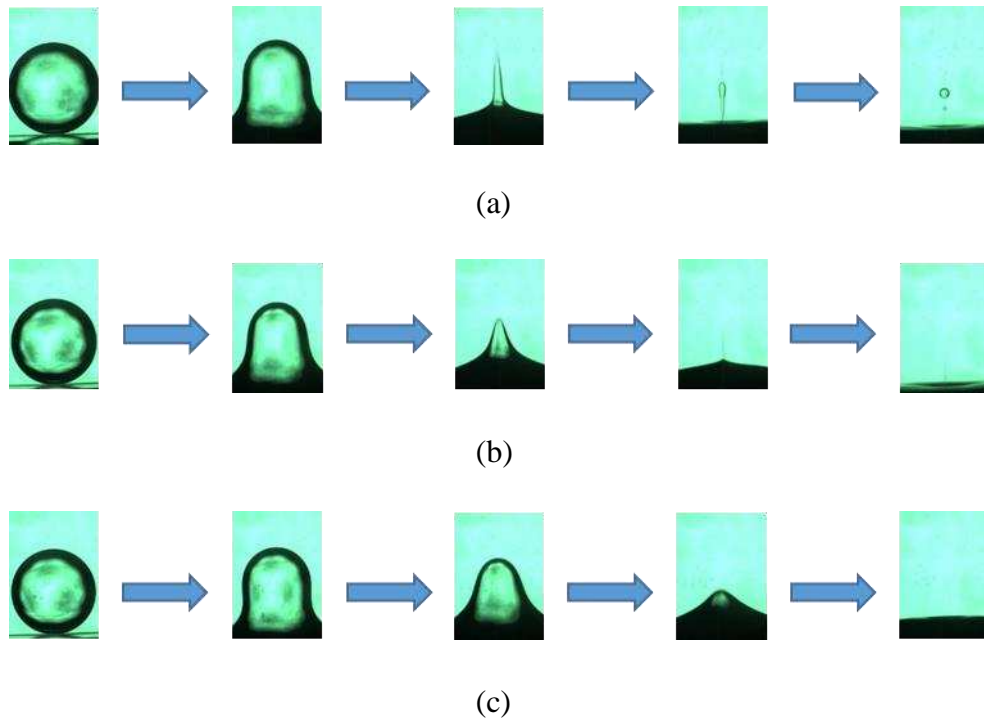


Fig. 10 Transformation from partial to complete coalescence by increasing frequency, for (a) 15 Hz, (b) 30 Hz, and (c) 50 Hz. (The initial droplet with a radius of  $640 \mu\text{m}$  under a PUDC electric field with an amplitude of  $400 \text{ kV}\cdot\text{m}^{-1}$ ; the concentration of HPAM solutions is 50 ppm)

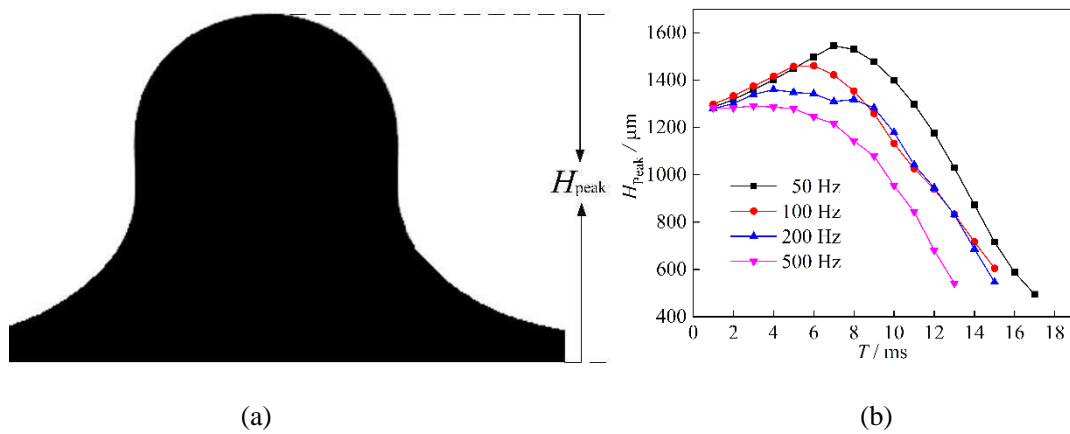


Fig. 11 (a) Schematic illustration of the distance ( $H_{\text{peak}}$ ) from the highest point of the coalescing droplet to the undeformed oil–water interface, and (b) Variations in the characteristic height of the droplet during coalescence for different frequencies. (The initial droplet with a radius of  $640 \mu\text{m}$  under a PUDC electric field with a amplitude of  $345 \text{ kV}\cdot\text{m}^{-1}$ ; the concentration of HPAM solutions

is 600 ppm)

As shown in Fig. 12 (a - d), the pattern of increase of  $E_{\text{crit}}$  depends on the waveform. In particular,  $E_{\text{crit}}$  of square waveform increases rapidly initially as frequency is increased from low values; however, it quickly approaches an asymptotic to the level when the frequency is increased above approximately 20 Hz. For sine AC and PUAC waveforms (Fig. 12 (b & c)),  $E_{\text{crit}}$  keeps increasing with frequencies, albeit at different rates. The change in  $E_{\text{crit}}$  of PUDC waveform (Fig. 12 (d)) is similar to those of sine AC waveform, i.e. with a change in the slope around 20 to 30 Hz. These strange changes in  $E_{\text{crit}}$  could not easily be explained, but maybe related to the natural frequency of polymer droplet given by [54]:

$$f_0 = C_f \cdot \frac{1}{\pi} \sqrt{\frac{\sigma}{(1+C_m)R^3\rho_w}}$$

where  $C_f$  and  $C_m$  are coefficients ( $C_f \approx 1$  and  $C_m \approx 1$ ). For polymer concentrations of 50, 100, 200, 400, and 600 ppm, the natural frequency ranges from 72.7 to 77.5 Hz for droplet radius of 640  $\mu\text{m}$ . The deformation should increase as the electric frequency tends to natural frequency of the droplet [54], conducive to breakup of the droplet and formation of secondary droplets. For square waveform,  $E_{\text{crit}}$  hardly changes over a wide range around the natural frequency. However, for sine AC, PUAC and PUDC waveforms  $E_{\text{crit}}$  remains almost unchanged at relatively low frequencies below 20 to 30 Hz. These results reveal the complexity of the effects of electric waveforms and frequencies. Under changing electric fields, the droplet is in a dynamic stretching mode, resulting in dynamic changes in the polymer molecules assembly structure. The behavior of polymer-solution droplets under changing electric fields is worthy of

further studies with focus on deformation and breakup.

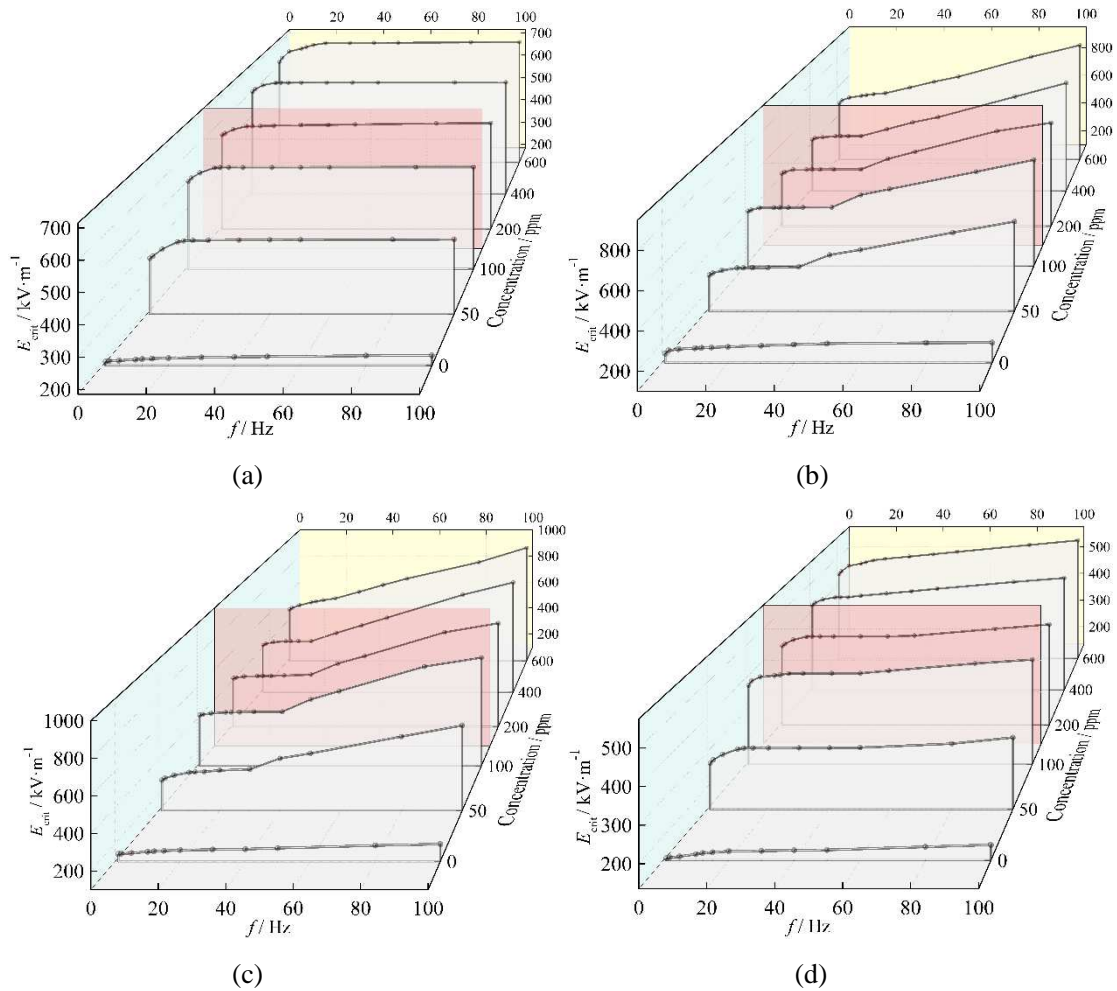


Fig. 12 Effect of electric field frequency on  $E_{crit}$  for droplets of polymer- solution of different concentrations: (a) square waveform, (b) sine AC waveform, (c) PUAC waveform, and (d) PUDC waveform. The initial droplet has a radius of  $640\ \mu\text{m}$ .

### 3.4 Effective waveforms for suppressing droplet–interface partial coalescence

High  $E_{crit}$  values are not conducive to the occurrence of partial coalescence. As the frequency is increased, the most effective waveform suppressing partial coalescence may also change. In Fig. 13 (a),  $E_{crit}$  of square waveform has the largest value of all tested frequencies, and the growth of  $E_{crit}$  of both sine AC or PUAC waveforms does not exceed that of square waveform. In Fig. 13 (b - f),  $E_{crit}$  of square

waveform is the largest at low frequencies; however,  $E_{\text{crit}}$  of sine AC and PUAC waveforms exceed that of square waveform at high frequencies. These results indicate that the most effective waveform may change from square to sine AC and PUAC waveforms at elevated frequencies. Furthermore,  $E_{\text{crit}}$  of PUDC waveform is always the lowest for different HPAM solution concentrations and frequencies.

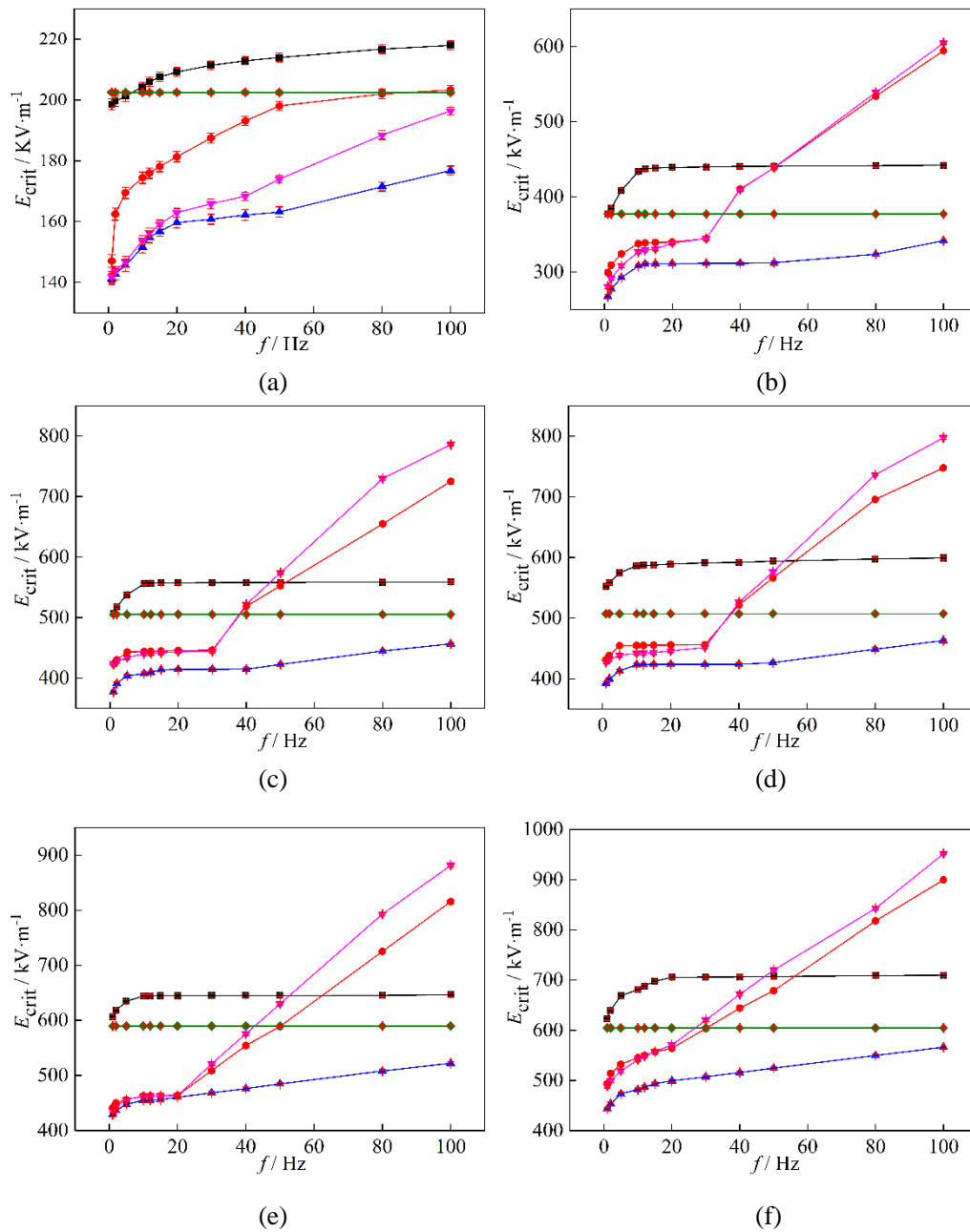


Fig. 13 Comparison of  $E_{\text{crit}}$  for different HPAM concentrations: (a) 0 ppm, (b) 50 ppm, (c) 100 ppm, (d) 200 ppm, (e) 400 ppm, and (f) 600 ppm. The values of  $E_{\text{crit}}$  of DC electric fields are

quoted from [28]. For legends, —■— represents square waveform, —◆— represents DC waveform, —●— represents sine AC, —▼— represents PUAC waveform, and —▲— represents PUDC waveform.

The change of the most effective waveform at high frequencies should be related to the difference in amplitude and average electric field strength of different waveforms. At low frequencies, the amplitude of electric field may have a greater influence on droplet–interface coalescence than the average electric field strength. From the periodic characteristics of different waveforms (Fig. 2 and Table. 2), the amplitude of electric field of PUDC, PUAC and sine AC waveforms is  $\sqrt{2}$  times that of DC and square waveforms at the same RMS value. In addition, the amplitude of sine AC waveform only appears at the peak and trough of the period, where duration is much less than that of PUDC and PUAC waveforms. Larger peak strength and longer duration would indicate that the droplet is subjected to stronger electric forces during coalescence, which could promote occurrence of partial coalescence. Therefore,  $E_{\text{crit}}$  values of DC and square waveforms are the largest, followed by sine AC, PUAC, and PUDC waveforms. As frequency increases, there will be several electric field periods throughout a whole coalescence time, so that the effect of average electric field strength during coalescence may become more significant. In particular, PUDC waveform electric fields vanish during the second half of one period. The disappearance of electric fields occurs twice for PUAC waveform in one period. During this time, the droplet is not affected by  $F_E$  during coalescence, favorable for occurrence of complete coalescence. At the same RMS value ( $E_0$ ), the average field

strength in one period for PUDC and PUAC waveforms is  $(\sqrt{2}/2) E_0$ . The average field strength in one period of sine AC waveform is  $(2\sqrt{2}/\pi) E_0$  and that of DC and square waveforms is  $E_0$ . When the frequency is high,  $E_{\text{crit}}$  values of PUAC and sine AC follow each other closely and exceed those of the square, DC and PUDC waveforms.

**Table 2 Theoretical RMS, peak and average strength values of different electric fields used in experiments [55]**

Waveform	$E_{\text{RMS}}$	$E_{\text{Peak}}$	$ E _{\text{Average}}$
PUDC	$E_0$	$\sqrt{2}E_0$	$(\sqrt{2}/2)E_0$
PUAC	$E_0$	$\sqrt{2}E_0$	$(\sqrt{2}/2)E_0$
Sine AC	$E_0$	$\sqrt{2}E_0$	$(2\sqrt{2}/\pi)E_0$
Bipolar Square	$E_0$	$E_0$	$E_0$

## Conclusions

In this study, the effect of Hydrolyzed Polyacrylamide (HPAM) polymer on droplet–interface electro-coalescence was studied using high-speed camera. Experimental results showed that increasing the applied electric field strength can transform the coalescence from complete to partial. Due to the viscoelasticity of droplet containing HPAM molecules, it was observed at relatively strong electric fields that the coalescing droplet was stretched to form a thin filament without pinch-off and fine droplets erupted from the summit of the filament. In view of the partial coalescence only initiates above a critical electric field ( $E_{\text{crit}}$ ), the values of  $E_{\text{crit}}$

were further determined.

The effects of the initial droplet size, HPAM solution concentration, electric field waveform and its frequency on  $E_{crit}$  were investigated. It was found that the increment of the initial droplet radius ( $R$ ) reduced the values of  $E_{crit}$ , and  $E_{crit}$  was nearly linear with  $R^{0.5}$ . Conversely, the addition of HPAM significantly increased  $E_{crit}$ , because of the increased viscoelasticity hindering droplet breakage as well as the change in physical properties of polymer solution (possibly mainly the increase in conductivity). In the experiments, the values of  $E_{crit}$  could rise from  $198.6 \text{ kV}\cdot\text{m}^{-1}$  (the coalescing droplet with a radius of  $640 \text{ }\mu\text{m}$  had a polymer concentration of  $0 \text{ ppm}$ ) to  $844.8 \text{ kV}\cdot\text{m}^{-1}$  (the coalescing droplet with a radius of  $470 \text{ }\mu\text{m}$  had a polymer concentration of  $600 \text{ ppm}$ ). Moreover, the results revealed that increasing frequency led to an increase in  $E_{crit}$ , which was related to the inhibition of the electro-induced stretching of droplets in the vertical direction. The maximum value of  $E_{crit}$  measured was approximately  $951.6 \text{ kV}\cdot\text{m}^{-1}$ , when the droplet with a radius of  $640 \text{ }\mu\text{m}$  (the polymer concentration was  $600 \text{ ppm}$ ) was in a pulsed AC electric field with frequency of  $100 \text{ Hz}$ . The increase in  $E_{crit}$  followed different ways for various waveforms. For square waveform,  $E_{crit}$  increased rapidly initially as frequency was increased and then approached an asymptotic to the level. However, for sine AC, PUAC, and PUDC waveforms,  $E_{crit}$  kept increasing with frequencies, albeit at different rates. Elevated values of  $E_{crit}$  led to most effective suppression of partial coalescence. In terms of the optimal waveform, the data revealed changes at elevated electric field frequencies. In most situations,  $E_{crit}$  of square waveform was the largest, but  $E_{crit}$  values of PUAC and

sine AC waveforms exceeded those of square waveform at high frequencies.

Overall, these results would form a good basis for future development of electric dehydration separators. However, the mechanism of breakage in thread and ejection of fine droplets from the summit under electric fields require further investigations. Furthermore, the influences of changes in electric field on the polymer molecules in aqueous solution and the resulting viscoelastic properties of droplets at high deformation frequencies remain unclear and require further studies.

### **Acknowledgements**

This work is supported by grants from the National Natural Science Foundation of China (Grant No. 51704318, 51674281), the Natural Science Foundation of Shandong Province, China (Grant No. ZR2017BEE008) and the Fundamental Research Funds for the Central Universities of China (Grant No. 19CX02033A). Introduction of Talent Research Start-up Fund (Grant No. YJ201601016), and the Scientific and Technology Planning Project of Gansu Province of China (Grant No. 18YF1GA006). It was carried out at the University of Leeds, where the first author stayed for a year as a visiting scholar. The authors would like to thank Drs Ali Hassanpour, Vincenzino Vivacqua, Umair Zafar and Mehrdad Pasha for their generous help and support.

### **References**

- [1] Kamal, M. S., Sultan, A.S., Almubaiyedh, U.A., Hussein, I.A., 2015. Review on Polymer Flooding: Rheology, Adsorption, Stability, and Field Applications of Various Polymer Systems. *Polym. Rev.* 21, 1-40.

- [2] Mogollon, J.L., Lokhandwala, T., 2013. Rejuvenating Viscous Oil Reservoirs by Polymer Injection: Lessons Learned in the Field, Paper presented at the SPE Enhanced Oil Recovery Conference, Kuala Lumpur, July 2-4. Society of Petroleum Engineers, SPE 165275.
- [3] Renouf, G., 2014. A Survey of Polymer Flooding in Western Canada, Paper presented at the SPE Improved Oil Recovery Symposium, Tulsa, April 12-16. Society of Petroleum Engineers, SPE 169062.
- [4] Sheng, J. J., Leonhardt, B., Azri, N., 2015. Status of Polymer-Flooding Technology. *J. Can. Petrol. Technol.* 54, 116-126.
- [5] Zhu, Y., Hou, Q., Liu, W., Ma, D., Liao, G.Z., 2013. Recent Progress and Effects Analysis of ASP Flooding Field Tests, Paper presented at the SPE Improved Oil Recovery Symposium, Tulsa, April 14-18. Society of Petroleum Engineers, SPE 151285.
- [6] Wang, D.M., Liang, C.J., Wu, J.Z., Wang, G., 2005. Application of polymer flooding technology in Daqing Oilfield. *Acta Petrol. Sin.* 26, 74-78.
- [7] Li, D.S., Kang, W.L., Zhu H.J., 2003. Study on Viscoelasticity of Polyacrylamide Solution. *Oilfield Chem.* 20, 347-350.
- [8] Eow, J.S., Ghadiri, M., Sharif, A.O., Williams, T.J., 2001. Electrostatic enhancement of coalescence of water droplets in oil: A review of the current understanding. *Chem. Eng. J.* 84, 173-192.
- [9] Sjöblom, J., 2001. *Encyclopedic Handbook of Emulsion Technology*, 2ed. Marcel Dekker, New York.
- [10] Zolfaghari, R., Fakhru'l-Razi, A., Abdullah, L.C., Elnashaie, S.S.E.H., Pendashteh, A., 2016. Demulsification techniques of water-in-oil and oil-in-water emulsions in petroleum industry.

Sep. Purif. Technol. 170, 377-407.

- [11] Eow, J.S., Ghadiri, M., 2002. Electrostatic enhancement of coalescence of water droplets in oil: a review of the technology. Chem. Eng. J. 85, 357-368.
- [12] Deng, S.B., Bai, R.B., Chen, J.P., Jiang, Z.P., Yu, G., Zhou, F.S., Chen, Z.X., 2002. Produced water from polymer flooding process in crude oil extraction: characterization and treatment by a novel crossflow oil–water separator. Sep. Purif. Technol. 29, 207-216.
- [13] Luo, X.M., Huang, X., Yan, H.P., Yang, D.H., Zhang, P.F., He, L.M., 2018. An experimental study on the coalescence behavior of oil droplet in ASP solution. Sep. Purif. Technol. 203, 152-158.
- [14] Eow, J.S., Ghadiri, M., 2002. Electrocoalesce-separators for the separation of aqueous drops from a flowing dielectric viscous liquid. Sep. Purif. Technol. 29, 63-77.
- [15] Chen, J.D., 1985. A Model of Coalescence between two Equal-Sized Spherical Drops of Bubbles. J. Colloid Interf. Sci. 107, 209-220.
- [16] Mousavichoubeh, M., Shariaty-Niassar, M., Ghadiri, M., 2011. The effect of interfacial tension on secondary drop formation in electro-coalescence of water droplets in oil. Chem. Eng. Sci. 66, 5330-5337.
- [17] Weheliye, W.H., Dong, T., Angeli, P., 2017. On the effect of surfactants on drop coalescence at liquid/liquid interfaces. Chem. Eng. Sci. 161, 215-227.
- [18] Eow, J.S., Ghadiri, M., 2003. Motion, deformation and break-up of aqueous drops in oils under high electric field strengths. Chem. Eng. Process. 42, 259-272.
- [19] Førdedal, H., Schildberg, Y., Sjöblom, J., Volle, J. L., 1996. Crude oil emulsions in high electric fields as studied by dielectric spectroscopy. Influence of interaction between

commercial and indigenous surfactants. *Colloids Surface. A* 106, 33–47.

- [20] Mohammadi, M., 2017. Numerical and experimental study on electric field driven coalescence of binary falling droplets in oil. *Sep. Purif. Technol.* 176, 262-276.
- [21] Blanchette, F., Bigioni, T.P., 2006. Partial coalescence of drops at liquid interfaces. *Nat. Phys.* 2, 254–257.
- [22] Aryafar, H., Kavehpour, H.P., 2006. Drop coalescence through planar surfaces. *Phys. Fluids* 18, 072105.
- [23] Aryafar, H., Kavehpour, H.P., 2009. Electrocoalescence: Effects of dc electric fields on coalescence of drops at planar interfaces. *Langmuir* 25, 12460-12465.
- [24] Hamlin, B.S., Creasey, J.C., Ristenpart, W.D., 2012. Electrically tunable partial coalescence of oppositely charged drops. *Phys. Rev. Lett.* 109, 6709-6717.
- [25] Mousavi, S.H., Ghadiri, M., Buckley, M., 2014. Electro-coalescence of water drops in oils under pulsatile electric fields. *Chem. Eng. Sci.* 120,130-142.
- [26] Mousavichoubeh, M., Ghadiri, M., M., Shariaty-Niassar, 2011. Electro-coalescence of an aqueous droplet at an oil–water interface. *Chem. Eng. Process.* 50, 338-344.
- [27] Vivacqua, V., Ghadiri, M., Abdullah, A.M., Hassanpour, A., Al-Marri, M.J., Azzopardi, B., Hewakandamby, B., Kermani, B., 2016. Analysis of partial electrocoalescence by level-set and finite element methods. *Chem. Eng. Res. Des.* 114, 180-189.
- [28] Yang, D.H., Ghadiri, M., Sun, Y.X., He, L.M., Luo, X.M., Lü, Y.L., 2018. Critical electric field strength for partial coalescence of droplets on oil–water interface under DC electric field. *Chem. Eng. Res. Des.* 136, 83-93.
- [29] Harbottle, D., Bueno, P., Isaksson, R., Kretschmar, I., 2011. Coalescence of particle-laden

- drops with a planar oil–water interface. *J. Colloid Interf. Sci.* 362, 235-241. doi: 10.1016/j.jcis.2011.05.077.
- [30] Vivacqua, V., Mhatre, S., Ghadiri, M., Abdullah, A.M., Hassanpour, A., Al-Marri, M.J., Azzopardi, B., Hewakandamby, B., Kermani, B., 2015. Electrocoalescence of water drop trains in oil under constant and pulsatile electric fields. *Chem. Eng. Res. Des.* 104, 658-668.
- [31] Luo, X.M., Huang, X., Yan, H.P., Yang, D.H., Zhang, P.F., He, L.M., 2018. An experimental study on the floating motion of oil drop in ASP solution. *Chem. Eng. Process.* 125, 97-104.
- [32] Yan, H.P., He, L.M., Luo, X.M., Wang, J., 2015. The study of deformation characteristics of polymer droplet under electric field. *Colloid Polym. Sci.* 293, 2045-2052.
- [33] Verdier, C., 2000. Coalescence of polymer droplets: experiments on collision. *CR. Phys.* 1, 119-126.
- [34] Lesaint, C., Glomm, W.R., Lundgaard, L.E., Sjöblom, J., 2009. Dehydration efficiency of AC electrical fields on water-in-model-oil emulsions, *Colloid. Surface A* 352, 63-69.
- [35] Lundgaard, L., Berg, G., Pedersen, A., Nielsen, P.J., 2002. Electrocoalescence of water drop pairs in oil, Paper presented at the Proceedings of 2002 IEEE 14th International Conference on Dielectric Liquids, Graz, Austria, Austria, July 12. IEEE, 7461765.
- [36] Drelich, J., Bryll, G., Kapczynski, J., Hupka, J., Miller, J.D., Hanson, F.V., 1992. The effect of electric field pulsation frequency on breaking water-in-oil emulsions. *Fuel Process. Technol.* 31, 105-113.
- [37] Ait-Kadi, A., Carreau, P.J., Chauveteau, G., 1987. Rheological Properties of Partially Hydrolyzed Polyacrylamide Solutions. *J. Rheol.* 31, 537-561.
- [38] Luo, X.M., Yin, H.R., Yan, H.P., Huang, X., Yang, D.H., He, L.M., 2018. The

electrocoalescence behavior of surfactant-laden droplet pairs in oil under a DC electric field.

Chem. Eng. Sci. 191, 350-257.

[39] Disna Jayampathi Karunanayake, K.P., Hoshino, Y., 2010. Electrostatic force acting on conductive ball between electrodes. J. Electrostat. 68, 91-95.

[40] Mhatre, S., Vivacqua, V., Ghadiri, M., Abdullah, A.M., Al-Marri, M.J., Hassanpour, A., Hewakandamby, B., Azzopardi, B., Kermani, B., 2015. Electrostatic phase separation: A review. Chem. Eng. Res. Des. 96, 177-195.

[41] Chiesa, M., Ingebrigtsen, S., Melheim, J.A., Hemmingsen, P.V., Hansen, E.B., Hestad, Ø, 2006. Investigation of the role of viscosity on electrocoalescence of water droplets in oil. Sep. Purif. Technol. 50, 267-277.

[42] Chen, X., Mandre, S., Feng, J.J., 2006. An experimental study of the coalescence between a drop and an interface in Newtonian and polymeric liquids. Phys. Fluids 18, 236.

[43] Li, J., Fontelos, M.A., 2003. Drop dynamics on the beads-on-string structure for viscoelastic jets: A numerical study. Phys. Fluids 15, 922-937.

[44] Bazilevskii, A.V., Rozhkov, A.N., 2014. Dynamics of capillary breakup of elastic jets. Fluid Dynam. 49, 827-843.

[45] Rayleigh, L., 1892. On the instability of a cylinder of viscous liquid under capillary force. Phil. Mag. 34, 145-154. Doi:10.1080/14786449208620301

[46] Tjahjadi, M., Stone, H.A., Ottino, J.M., 1992. Satellite and subsatellite formation in capillary breakup. J. Fluid Mech. 243, 297-317.

[47] Kowalewski, T.A., 1996. On the separation of droplets from a liquid jet. Fluid Dyn. Res. 17, 121-145.

- [48] Stone, H.A., Bentley, B.J., Leal, L.G., 1986. An experimental study of transient effects in the breakup of viscous drops. *J. Fluid Mech.* 173, 131-158.
- [49] Stone, H.A., Leal, L.G., 1989. Relaxation and breakup of an initially extended drop in an otherwise quiescent fluid. *J. Fluid Mech.* 198, 299-427.
- [50] Amarouchen, Y., Bonn, D., Meunier, J., Kellay, H., 2001. Inhibition of the finite-time singularity during the droplet fission of a polymeric fluid. *Phys. Rev. Lett.* 86, 3558-3561.
- [51] Goldin, M., Yerushalmi, J., Pfeffer, R., Shinnar, R., 1969. Breakup of a laminar capillary jet of a viscoelastic fluid. *J. Fluid Mech.* 38, 689-711.
- [52] Hohman, M.M., Shin, M., Rutledge, G., Brenner, M.P., 2001. Electrospinning and electrically forced jets, II. Applications. *Phys. Fluids* 13, 2221-36.
- [53] Yue, P., Zhou, C., Feng, J.J., 2006. A computational study of the coalescence between a drop and an interface in Newtonian and viscoelastic fluids. *Phys. Fluids* 18, 102102.
- [54] He, L.M., Yan, H.P., Luo, X.M., Wang, J., Huang, X., Cao, J.H., Yang, D.H., 2016. An experimental investigation on the deformation of alkali-surfactant-polymer droplet under AC electric field. *Colloid Polym. Sci.* 294, 1-8.
- [55] Yang, D.H., Sun, Y.X., He, L.M., Luo, X.M., Lü, Y.L., Gao, Q.F., 2019. Partial coalescence of droplets at oil-water interface subjected to different electric waveforms: Effects of non-ionic surfactant on critical electric field strength. *Chem. Eng. Res. Des.* 142, 214-224.